VIBRATIONAL ENERGY TRANSFER PATHWAYS IN CH_3F UNDER WEAK AND STRONG EXCITATION CONDITIONS: A COMPARISON

V.A. APKARIAN, J.M. LINDQUIST
Department of Chemistry, University of California, Irvine, California 92717, USA

and

Eric WEITZ [1]
Department of Chemistry, Northwestern University, Evanston, Illinois 60201, USA

Received 30 May 1984; in final form 26 September 1984

Energy transfer processes in CH_3F have been reinvestigated under high excitation conditions with and without added rare gas via a mathematical model developed as a consequence of studies under low excitation. The model can be used to describe energy transfer under high excitation conditions with the inclusion of an additional state and energy transfer pathways coupling that state to others in the model. A conclusion using this model is that population from $3\nu_3$ does not significantly fill ν_1/ν_4 or $2(\nu_2/\nu_5)$ even in the high excitation regime. It is also concluded that multiple photon absorption takes place under high excitation conditions.

1. Introduction

Studies of vibrational energy transfer in CH_3F have been extensive and detailed [1–8]. The dominant pathways for energy transfer under low levels of excitation have been discerned and the appropriate rate constants measured [1–5]. As such CH_3F is considered a model polyatomic molecule with respect to vibrational energy transfer studies.

Recently, CH_3F has been studied under high excitation conditions using a TEA or focused, Q-switched CO_2 laser as the excitation source [4,6–8]. In these studies, temporal profiles for fluorescence emission from various CH_3F vibrational states differ from the case of mild excitation. In one set of experiments V → V processes in CH_3F were studied as a function of fluence and added rare gas [7,8]. An apparent conclusion of these studies was that some energy transfer pathways, unimportant at low levels of excitation, were important under high excitation conditions. These studies also concluded that the C–H stretching modes, ν_1/ν_4, are directly coupled and efficiently populated from the second C–F stretching overtone, $3\nu_3$. $3\nu_3$ is also postulated as the source of population for the C–H bending overtones $2(\nu_2/\nu_5)$. These conclusions, based on the observation of fast risetimes of ν_1/ν_4 and $2(\nu_2/\nu_5)$, which are dependent on the degree of CH_3F excitation, are contrary to those derived from a number of studies of energy transfer in CH_3F under low excitation conditions [1–5].

The present investigation is an effort to determine if new energy transfer pathways do become important under high excitation conditions and in particular to determine whether the $3\nu_3 \rightarrow \nu_1/\nu_4 \rightarrow 2(\nu_2/\nu_5)$ pathway is significant at high levels of excitation. The focus of this investigation is a mathematical model of the energy transfer pathways in CH_3F which reproduces the behavior of all observed CH_3F vibrational states under low excitation conditions both with and without added rare gas [5].

[1] 1983–84 Visiting Fellow, Joint Institute for Laboratory Astrophysics, University of Colorado and National Bureau of Standards, Boulder, Colorado, USA.

0 009-2614/84/$ 03.00

2. The model

The model used to describe energy transfer in CH_3F under low levels of excitation is discussed in detail in ref. [5] with the relevant energy levels in fig. 1a. The model contains eight energy levels tied together by the kinetic processes

$$CH_3F(\nu_3) + M \underset{}{\overset{k_{36}}{\rightleftharpoons}} CH_3F(\nu_6) + M \quad (\Delta E = 133\ \mathrm{cm}^{-1}),$$
$$k_{36} = 294 \pm 27\ \mathrm{ms}^{-1}\ \mathrm{Torr}^{-1},$$
$$k_{36'} = 12 \pm 2\ \mathrm{ms}^{-1}\ (\mathrm{Torr\ Ar})^{-1}; \qquad (1)$$

$$CH_3F(\nu_6) + M \overset{k_{62}}{\rightleftharpoons} CH_3F(\nu_2,\nu_5) + M$$
$$(\Delta E = 284\ \mathrm{cm}^{-1}),$$
$$k_{62} = 70 \pm 17\ \mathrm{ms}^{-1}\ \mathrm{Torr}^{-1},$$
$$k_{62'} = 40 \pm 25\ \mathrm{ms}^{-1}\ (\mathrm{Torr\ Ar})^{-1}; \qquad (2)$$

$$2CH_3F(\nu_3) \overset{k_{UL3}}{\rightleftharpoons} CH_3F(2\nu_3) + CH_3F(0)$$
$$(\Delta E \approx 0),$$
$$k_{UL3} = 2430 \pm 100\ \mathrm{ms}^{-1}\ \mathrm{Torr}^{-1}; \qquad (3)$$

$$CH_3F(\nu_3) + CH_3F(2\nu_3) \overset{k_{2UL3}}{\rightleftharpoons} CH_3F(3\nu_3) + CH_3F(0)$$
$$(\Delta E \approx 0),$$
$$k_{2UL3} = k_{UL3}; \qquad (4)$$

$$CH_3F(3\nu_3) + M \overset{k_{C2}}{\rightleftharpoons} CH_3F([\nu_1,\nu_4]) + M$$
$$(\Delta E = -170\ \mathrm{cm}^{-1}),$$
$$k_{C2} = k_{C1}, \quad k_{C2'} \leqslant k_{C1'}; \qquad (5)$$

$$2CH_3F([\nu_2,\nu_5]) \overset{k_{UL2}}{\rightleftharpoons} CH_3F(2[\nu_2,\nu_5]) + CH_3F(0)$$
$$(\Delta E \approx 0),$$
$$k_{UL2} = 1600 \pm 200\ \mathrm{ms}^{-1}\ \mathrm{Torr}^{-1}; \qquad (6)$$

$$CH_3F(2[\nu_2,\nu_5]) + M \overset{k_{C1}}{\rightleftharpoons} CH_3F([\nu_1,\nu_4]) + M$$
$$(\Delta E = 50\ \mathrm{cm}^{-1}),$$
$$k_{C1} = 300\ \mathrm{ms}^{-1}\ \mathrm{Torr}^{-1},$$
$$k_{C1'} = 130 \pm 30\ \mathrm{ms}^{-1}\ (\mathrm{Torr\ Ar})^{-1}, \qquad (7)$$

with rate constants as indicated. Primes refer to rare-gas-dependent rate constants. A firm conclusion of

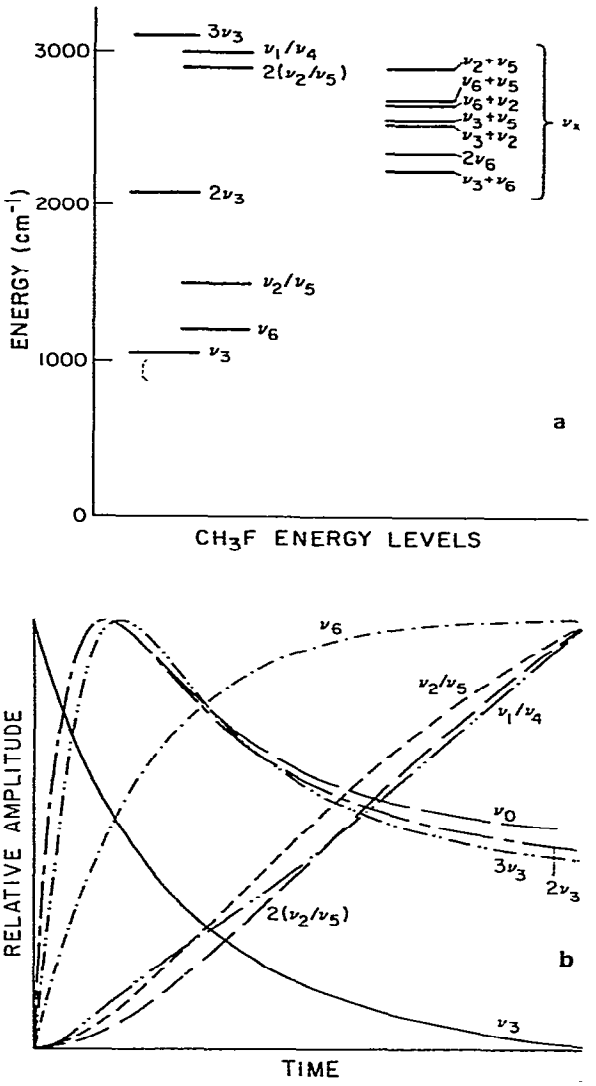

Fig. 1. (a) Energy level diagram for CH_3F. Shown on the left are the states that compose the eight-level model for CH_3F. Shown on the right are the combination and overtone states in the 2000–3000 cm^{-1} region and the location of the composite state designated as ν_x in the nine-level model. (b) Evolution of population in the states in the eight-level model. The rate equations were integrated for the situation where 1% of the ground-state population in a 0.06 Torr sample of CH_3F was transferred to ν_3. $t = 0$ occurs after the laser pulse has populated the appropriate states. The total time base is 12.5 μs. Note that the amplitudes of all curves in figs. (1b)–(4) are individually normalized on the timescale shown. Thus, the same amplitude on different curves can represent a different population.

this model is, under low excitation conditions corresponding to transfer of ≈1% or less of the ground-state population to ν_3, energy transfer from $3\nu_3$ to ν_1/ν_4 does not play a major role in populating ν_1/ν_4. An explanation for this is that population filling ν_1/ν_4 from $3\nu_3$ involves trying to fill a state with a large population reservoir from a state with a small population reservoir. As discussed in ref. [5] this is an unfavorable case for efficiently populating a state. The situation becomes worse when the coupling of ν_1/ν_4 to $2(\nu_2/\nu_5)$ is included as this increases the effective heat capacity of the states to be populated through $3\nu_3$. Under these circumstances, the rate of filling of the higher heat capacity state is slowed relative to the rate constant connecting the two states [5]. The magnitude of the effect is approximately given by the population of the intermediate (bottleneck) state ($3\nu_3$) divided by the sum of the populations of the intermediate and final states (ν_1/ν_4 and $2(\nu_2/\nu_5)$). This does not imply that $3\nu_3$ cannot contribute to the filling of ν_2/ν_5 since a non-zero rate constant connects these states. However, if the rate constant connecting $3\nu_3$ to ν_1/ν_4 is increased so that $3\nu_3$ fills ν_1/ν_4 significantly (≈10%), then the temporal rise of the ν_1/ν_4 signal develops a fast initial bump which is not seen experimentally under low excitation conditions. Hence, it was concluded that the rate constant for population transfer from $3\nu_3$ to ν_1/ν_4, k_{C2} in the model, could not significantly exceed the rate constant for population transfer from $2(\nu_2/\nu_5)$ to ν_1/ν_4, k_{C1}. The value of $k_{C1'}$ was established by other considerations as 130 ± 30 ms^{-1} $(Torr\ Ar)^{-1}$. The lower limits for $k_{C1'}$ and upper limits for $k_{C2'}$ as a function of argon pressure were also determined. These rate constants produced excellent agreement between generated and experimental signals for all observed states over a wide range of parent and rare gas pressures for studies done at low excitation. *Since the kinetic equations for a given system, if correct, are valid for any excitation level and rate constants are not a function of level of excitation, a complete and accurate kinetic model should be accurate in any excitation regime.* It is possible that a given channel will grow in importance as the level of excitation increases since energy transfer pathways contain steps that are both linear and non-linear in the degree of excitation. Thus, a new channel unimportant at low excitation may have to be included in the model to account for observations under high excitation conditions. However, while observed *rates* for a process may change as a function of initial excitation conditions, *rate constants are not a function of the level or distribution of initial excitation.*

The work in refs. [7,8] involves strong pumping of CH_3F with various amounts of added rare gas. The results in these references served as the basis for comparison with the predictions of the model. However, under high excitation conditions, unlike the low excitation case, the initial state preparation of the molecule is unknown. Direct population of upper states via multiple photon absorption through rotational resonances induced by collisional redistribution is expected. However, neither the states involved nor the degree of excitation is known. Thus, there are enough free parameters in the model with insufficient experimental observations that agreement between generated signals and experimental data is not unique. As such, we chose to concentrate on obtaining a qualitative understanding of the differences in kinetics in the high and low excitation regimes.

3. Results and discussion

A plot of the population versus time for all eight levels at low excitation is shown in fig. 1b. These signals are generated for 1% of the ground-state molecules in a 0.6 Torr sample of CH_3F being pumped to the ν_3 level. All states behave as expected with the ν_3 manifold equilibrating on the fastest timescale [1–5]. The ν_3 manifold then successively equilibrates with ν_6 and ν_2/ν_5 [4]. The 3μ states, $2(\nu_2/\nu_5)$ and ν_1/ν_4, are then populated from ν_2/ν_5. The populations of these upper states are too small to perceptibly affect the populations of the states at or below 2000 cm^{-1}, and therefore no obvious change is observed in the populations of the lower states as they equilibrate with the 3000 cm^{-1} states.

To simulate high excitation conditions, a pump efficiency of 40% was arbitrarily assumed, i.e. the rate equations were integrated subject to the initial condition; at $t = 0$ (after the laser pulse), $N_{\nu_3} = N^0_{\nu_3} + 0.4N^0_0$ and $N_0 = 0.6N^0_0$ (where N^0_i is the ambient population of state i). Fig. 2a illustrates this situation for a CH_3F pressure of 0.6 Torr. In comparison with fig. 1b, ν_1/ν_4 is now populated much more rapidly. Clearly much of the population feeding into ν_1/ν_4 must come from $3\nu_3$

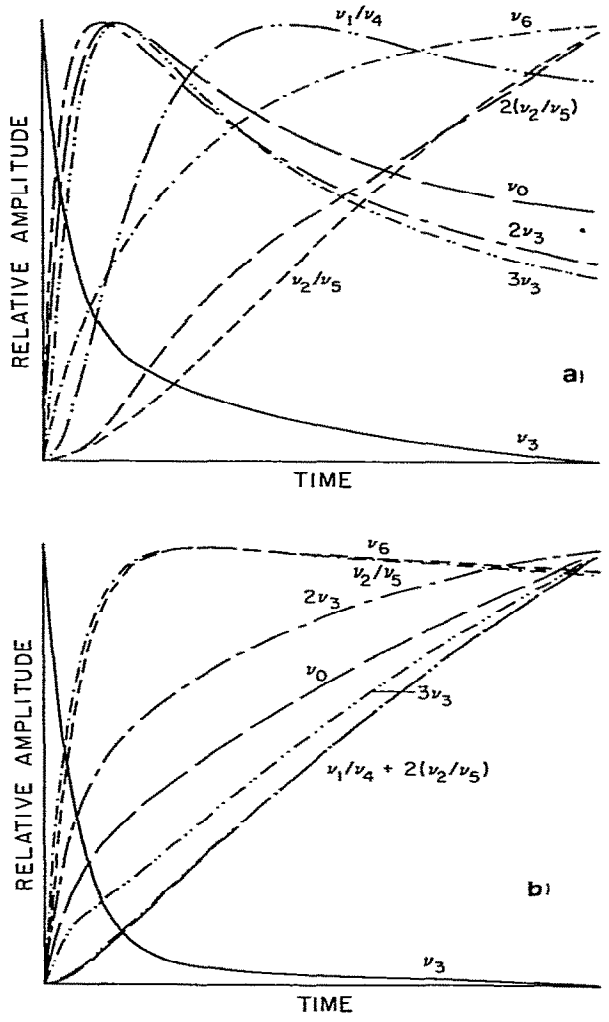

Fig. 2. The rate equations are integrated for a strong laser pump where 40% of the ground-state population is transferred to ν_3. (a) 0.6 Torr sample of CH_3F and (b) 0.06 Torr CH_3F + 70 Torr argon. All else is as for fig. 1.

since $2(\nu_2/\nu_5)$ is still populated at approximately the same rate as in fig. 1b. These features illustrate an important recurring point. With a 40% pump, the ν_3 manifold equilibrates at a very high vibrational temperature. (A relative population of 0.66 for ν_3/ground corresponds to a ≈3000 K vibrational temperature.) Under these circumstances $3\nu_3$ is very highly excited. In fact, due to the exothermicity of up-pumping steps, its vibrational temperature would be expected to be higher relative to the ground state than the temperature of ν_3 [2]. With this large population, $3\nu_3$ can now significantly fill ν_1/ν_4. However, even in these circumstances, the vibrational heat capacity of $2(\nu_2/\nu_5)$ is too large for $3\nu_3$ to fill it. $2(\nu_2/\nu_5)$ does have an early fast bump which is due to filling from $3\nu_3$. However, $3\nu_3$ does not have the population to fill $2(\nu_2/\nu_5)$ to its equilibrium value. Furthermore, the ν_3 manifold equilibrates with the rest of the vibrational states most efficiently through the pathway $\nu_3 \rightarrow \nu_6 \rightarrow \nu_2/\nu_5$. This process manifests itself in the ν_3 manifold states and to a lesser extent in ν_1/ν_4 by the fast fall in their temporal profiles [4]. The filling of $2(\nu_2/\nu_5)$ via this channel is verified by the observation that $2(\nu_2/\nu_5)$ rises at virtually the same rate as (ν_2/ν_5). In comparison with experiment, while the appropriate ν_1/ν_4 behavior is reproduced, experimentally $2\nu_5$ is seen to rise with almost the rise time of ν_1/ν_4 and stays fairly flat on a V → V timescale [7,8]. The model does not reproduce this.

While this set of conditions reproduces the fast ν_1/ν_4 rise observed in pure CH_3F, it fails even for ν_1/ν_4 at lower CH_3F pressure with a high pressure of rare gas. Experimentally, detector limited rises are observed from $2\nu_3$ and ν_1/ν_4 for 0.06 Torr CH_3F mixed with 70 Torr Ar [7,8]. This is not possible in the current model with only a ν_3 pump, independent of the level of initial excitation. This failure can easily be understood. At low CH_3F and high Ar pressure, the nonlinear processes such as those in eqs. (3), (4) and (6) are slow compared to processes that can be induced by collision with Ar such as those of eqs. (1), (2) and (5), (7). According to the model the 3μ states are only accessible through non-linear steps; steps which require the collision of two excited CH_3F molecules. This can be observed in fig. 2b where ν_6 and ν_2/ν_5 are the only states to show a fast risetime. It is possible that a new pathway such as

$$CH_3F(\nu_2/\nu_5) + Ar \rightarrow CH_3F(2\nu_3) + Ar \qquad (8)$$

would open up. However, this is not likely at this argon pressure. The process of eq. (8) requires a three-quantum-number change and is of larger energy gap than the other non-resonant V → V processes in the system and thus would be expected to be much slower. With the data of refs. [7,8] and their quoted experimental response time, it is possible to deter-

mine that if the rise is due to a collisional process, then the rate constant for this process would have to be $\gtrsim 45$ ms^{-1} (Torr Ar)$^{-1}$. This is comparable to or slightly faster than the argon dependent rate constant for process (2) which connects ν_6 with ν_2/ν_5. Process (2) involves an energy gap of 300 cm^{-1} versus $\approx$500 cm^{-1} for the ν_2/ν_5 to $2\nu_3$ process and involves a two- versus three-quantum-number change. In fact, since the rate constant for equilibration of ν_3 with ν_6 is only 12 ms^{-1} (Torr Ar)$^{-1}$, even ν_2/ν_5 will not rise on the necessary timescale. Moreover, even if $2\nu_3$ was populated on this fast timescale, efficient, argon dependent channels would still have to be invoked in the transfer of population from $2\nu_3 \rightarrow 2(\nu_2/\nu_5)$, ν_1/ν_4. One is thus forced to conclude that, under these experimental conditions, the fast rises of $2\nu_3$, $2(\nu_2/\nu_5)$ and ν_1/ν_4 and the argon pressure dependence of these rises must involve the absorption of additional photons starting from ν_3 and other populated states.

For a 1.2 J/cm^2 laser pulse there are enough photons per molecule to saturate the ground to ν_3 transition in CH_3F [1]. There are also enough photons that sequential absorption of photons is possible and likely, particularly with added inert gas to speed up rotational equilibration. Since it is not likely that the absorption coefficient remains constant, we chose a 40% pump of molecules out of the ground state as our typical condition. We also somewhat arbitrarily designated that 10% of these molecules were up pumped to $2\nu_3$ and 10% of these molecules were up pumped to $3\nu_3$ as typical conditions for multiple photon up pumping (i.e. the initial conditions; at $t = 0$, $N_0 = 0.6N_0^0$, $N_{\nu_3} = N_{\nu_3}^0 + 0.36N_0^0$, $N_{2\nu_3} = N_{2\nu_3}^0 + 0.036N_0^0$, $N_{3\nu_3} = N_{3\nu_3}^0 + 0.004N_0^0$). Excitation of hot bands starting from ν_6 and ν_2/ν_5 is also likely but inclusion of these processes in the model would have required the choice of a large number of arbitrary parameters dealing with initial preparation of the system. As such hot band excitation of this type was not included in the model. To determine that observed effects were not a strong function of the degree of pumping or the distribution of molecules among the ν_3 manifold, we varied our pump conditions between a fully saturated ν_3 manifold and low excitation of just ν_3. Where observations were a function of the degree of pumping or the distribution of quanta among the ν_3 states, the dependence of the temporal evolution of a state as a function of excitation will be commented on.

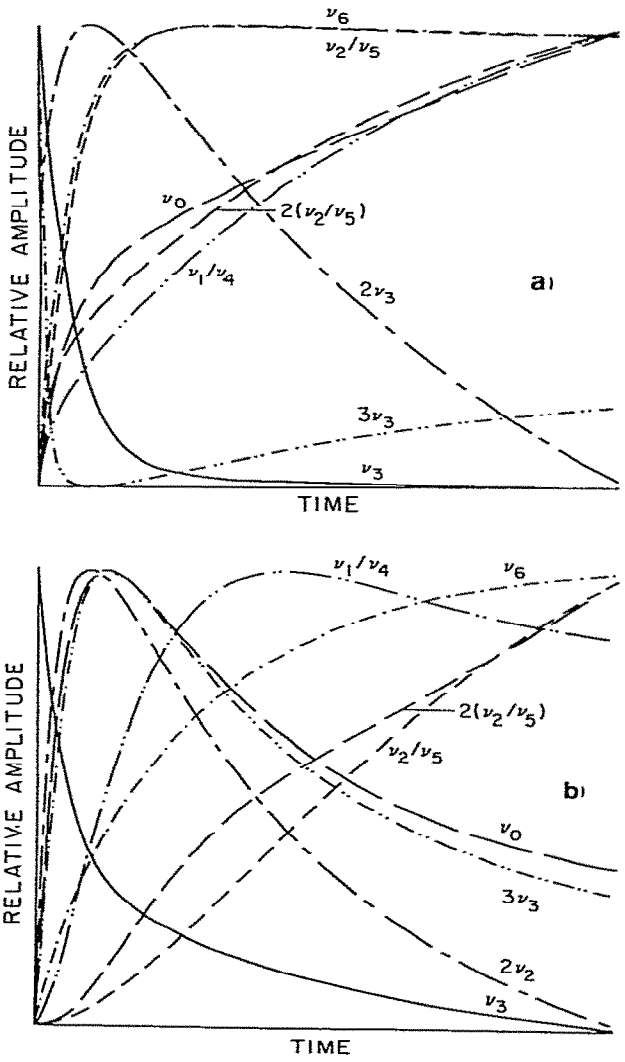

Fig. 3. The rate equations are integrated for a strong multiple pump where initial conditions are: $N_{\nu_3}^0 = N_{\nu_3}^0 + 0.36N_0^0$, $N_{2\nu_3} = N_{2\nu_3}^0 + 0.036N_0^0$ and $N_{3\nu_3} = N_{3\nu_3}^0 + 0.004N_0^0$. (a) 0.06 Torr CH_3F + 70 Torr Ar and (b) 0.6 Torr CH_3F. All else is as in figs. 1 and 2.

Signals generated with multiple pumping are shown in figs. 3a and 3b. In both cases the behavior of the generated signals is not compatible with a rapid rise of $2(\nu_2/\nu_5)$. Even with direct pumping of ν_3 overtones, the relative heat capacities of $2(\nu_2/\nu_5)$ versus $3\nu_3$ and the equilibration of the ν_3 manifold with the ν_6 and ν_2/ν_5 states prevents rapid population of $2(\nu_2/\nu_5)$ to

an equilibrium value. The rapid depletion of the ν_3 manifold in figs. 3a and 3b is due to the overpopulation of these states relative to their equilibrium population following the laser pulse. As seen in fig. 3a, for $3\nu_3$, the population in a state can also decrease and then increase. For $3\nu_3$ the depletion occurs as population is drained out of the ν_3 manifold to other states. Then, as $2(\nu_2/\nu_5)$ and (ν_1/ν_4) fill from (ν_2/ν_5), $3\nu_3$ is underpopulated relative to its ultimate equilibrium population and is refilled from $2(\nu_2/\nu_5)$ and (ν_1/ν_4). As seen in fig. 3a, even with multiple pumping, the addition of 70 Torr of argon to 0.06 Torr CH_3F does not change the situation in regard to ν_1/ν_4 and $2(\nu_2/\nu_5)$.

It is thus apparent that populating $2(\nu_2/\nu_5)$, and to a lesser extent ν_1/ν_4, to their equilibrium values in a rapid process requires collisional coupling of these states to one of high heat capacity. This immediately suggests a pathway where $2\nu_3$ is collisionally coupled to $2(\nu_2/\nu_5)$. If this process is fast enough, it will completely eliminate any heat capacity problems since $2\nu_3$ has a much higher heat capacity than $2(\nu_2/\nu_5)$ and thus the $2(\nu_2/\nu_5)$ population will be driven by the $2\nu_3$ population. This was accomplished in the model by including a multiply degenerate state at 2216 cm^{-1} which accounts for the total heat capacity of all combination bands and overtones in the 2000–3000 cm^{-1} region. This state designated as ν_x is coupled to other states via the pathway $2\nu_3 \rightarrow \nu_x \rightarrow 2(\nu_2/\nu_5)$. A rapid process of this type is more likely than a rapid process of the type $\nu_2/\nu_5 \rightarrow 2\nu_3$ because there are many intermediate states in the 2000 → 3000 cm^{-1} region which can be used as "rungs of a ladder" to go from 2000 → 3000 cm^{-1} via successive steps of small energy gap. Additionally, if hot band absorptions of the type $\nu_6 + h\nu \rightarrow \nu_3 + \nu_6$ and $\nu_2/\nu_5 + h\nu \rightarrow \nu_3 + (\nu_2/\nu_5)$ are invoked, the total energy necessary to go from these states to the 3000 cm^{-1} state diminishes and the overall process would be expected to be even faster. The high density of states in this region, their likely overlap and mixing and the smaller energy gap steps involved in going from ν_x to $2(\nu_2/\nu_5)$ would be expected to effectively mitigate the lack of propensity for multiple quantum transitions discussed previously in relation to coupling between (ν_2/ν_5) and $2\nu_3$.

Signals generated with rapid energy transfer among the 2000 → 3000 cm^{-1} manifold of states are shown in fig. 4 for the same distribution of initial population

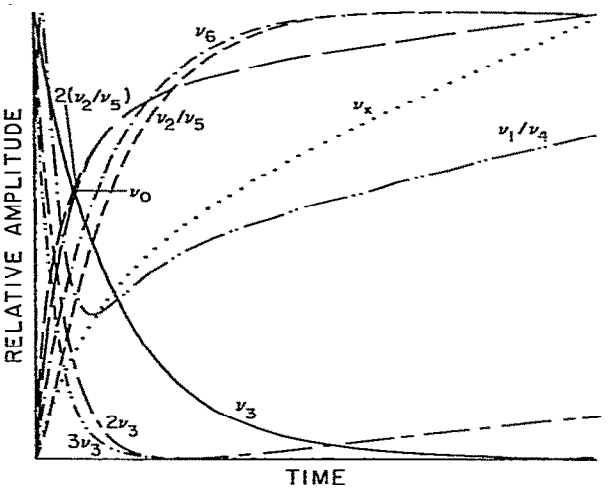

Fig. 4. The rate equations are integrated for the same sample and initial population conditions as in fig. 3a except the integrated equations are now for a nine-level model including the states of the eight-level model and ν_x.

in fig. 3a. Note the dramatic differences in the behavior of ν_1/ν_4 and $2(\nu_2/\nu_5)$ in fig. 4 versus fig. 3a. $2(\nu_2/\nu_5)$ fills to its equilibrium population and stays filled. ν_1/ν_4 is first filled from $3\nu_3$, then drops very rapidly as the ν_3 manifold is depleted and then refills through $2(\nu_2/\nu_5)$. The exact amplitude of the initial filling and fall of ν_1/ν_4 will depend on the distribution of initial excitation and the choice of rate constants coupling ν_x with $2\nu_3$ and $2(\nu_2/\nu_5)$. The initial fill and fall steps all occur within $\approx 1/2$ μs; thus, even if the actual initial conditions caused these effects to occur, they would be obscured in the reported experiments by the finite laser pulse width and electronic response time. What would be observed is the desired initial rapid rise of ν_1/ν_4 with a subsequent slower evolution of population. It is clear that the behavior of ν_1/ν_4 and $2(\nu_2/\nu_5)$ illustrated in fig. 4 *requires* coupling of these states to a state of large vibrational heat capacity that is filled rapidly. In our model this state is ν_x which is filled via $2\nu_3$. However, the available experimental data do not allow a firm assignment for ν_x.

As previously mentioned, direct photoexcitation to $\nu_0 + \nu_3$, and $\nu_2/\nu_5 + \nu_3$ is likely to occur under high fluence conditions. These processes would populate states of high vibrational heat capacity in the 2000 cm^{-1} region, identified in the model as ν_x. An-

other factor lending credence to hot band excitation is that when only the ν_3 manifold is pumped in the model, we observe the $2\nu_3$ and $3\nu_3$ temporal profiles depend strongly on the degree of pumping. If these states are initially overpopulated relative to their final populations at vibrational equilibrium, their populations will drop rapidly to equilibrium levels. If they are underpopulated, they will be fed from ν_3 and their populations will increase. $2\nu_3$ is reported to always stay near its equilibrium population following the pump pulse after sufficient argon is added to the system [7,8]. Since additional argon should affect the degree of up pumping, it seems likely that multiple photon absorption occurs via a variety of channels. Under these circumstances, there would be a greater tendency to distribute population over a number of molecular levels so that the ν_3 manifold would not have to donate a significant fraction of its population to other modes.

4. Conclusion

The eight-level kinetic model developed to describe energy transfer in CH_3F at low levels of excitation can be modified to model energy transfer at high levels of excitation. A state in the 2000–3000 cm^{-1} region is introduced which corresponds to the $\nu_3 + \nu_6$, $\nu_2/\nu_5 + \nu_3$, $\nu_2/\nu_5 + \nu_6$ and $2\nu_6$ states. This state is coupled to the $2\nu_3$ state and the $2(\nu_2/\nu_5)$ states and provides a pathway for coupling a state with large vibrational heat capacity, $2\nu_3$, to the 3000 cm^{-1} states. $3\nu_3$ cannot significantly contribute to the filling of $2(\nu_2/\nu_5)$ in *either the low or high excitation regime.* Direct multiple photon up pumping in CH_3F, under high fluence conditions, populates a number of states in addition to ν_3. The rapid rise observed for the states in the 3μ region under conditions of high fluence with and without added rare gas can be explained by this mechanism.

Acknowledgement

We would like to thank George Flynn for his encouragement to carry out this study and for many useful comments and discussions. Support of the National Science Foundation under grant CHE82-06976 is appreciated (EW). Support of the Camille and Henry Dreyfus Foundation via a "Newly Appointed Young Faculty in Chemistry" award is acknowledged (VAA).

References

[1] E. Weitz and G.W. Flynn, J. Chem. Phys. 58 (1973) 2781.
[2] E. Weitz and G.W. Flynn, in: Photoselective chemistry, Part II. Advances in chemsitry series, Vol. 47, eds. J. Jortner, R.D. Levine and S.A. Rice (Wiley–Interscience, New York, 1981) p. 185.
[3] R.E. McNair, S.F. Fulghum, G.W. Flynn, M.S. Feld and B.J. Feldman, Chem. Phys. Letters 48 (1977) 241;
F.R. Grabiner, G.W. Flynn and A.M. Ronn, J. Chem. Phys. 59 (1973) 2330;
I. Shamah and G.W. Flynn, J. Chem. Phys. 69 (1978) 2330;
J.M. Preses, G.W. Flynn and E. Weitz, J. Chem. Phys. 69 (1978) 2782.
[4] R.S. Sheory and G.W. Flynn, J. Chem. Phys. 72 (1980) 1175.
[5] V.A. Apkarian and E. Weitz, J. Chem. Phys. 71 (1979) 4349.
[6] M. Kneba and J. Wolfrum, Ber. Bunsenges. Physik, Chem. 81 (1977) 1275.
[7] H. Nakane and S. Tsuchiya, Chem. Phys. Letters 80 (1981) 458.
[8] H. Nakane and S. Tsuchiya, Chem. Phys. Letters 84 (1981) 322.